ARTICLE TYPE

Enhanced Electrical Conductivities of N-doped Carbon Nanotubes by Controlled Heat Treatments

Kazunori Fujisawa,[a] Tomohiro Tojo,[a] Hiroyuki Muramatsu,[b] Ana L. Elías,[d] Sofía M. Vega-Díaz,[c] Ferdinando Tristán-López,[c] Jin Hee Kim,[a] Takuya Hayashi,[a] Yoong Ahm Kim,[a]* Morinobu Endo,[a,b,c] and
5 **Mauricio Terrones[c,d]**

The thermal stability of nitrogen (N) functionalities on the sidewalls of N-doped multi-walled carbon nanotubes was investigated at temperatures ranging between 1000 °C and 2000 °C. The structural
10 stability of the doped tubes was then correlated to the electrical conductivity both at the bulk and at the individual tube levels. When as-grown tubes were thermally treated at 1000 °C, we observed a very significant decrease in the electrical resistance of the individual nanotubes, from 54 kΩ to 0.5 kΩ, which is attributed to a low N doping level (e.g. 0.78 at % N). We noted that pyridine-type N was first decomposed whereas the substitutional N was stable up to 1500 °C. For nanotubes heat treated to 1800 °C
15 and 2000 °C, the tubes exhibited an improved degree of crystallinity which was confirmed by both the low R value (I_D/I_G) in the Raman spectra, and the presence of straight graphitic planes observed in TEM images. However, N atoms were not detected in these tubes and caused an increase in their electrical resistivity and resistance. These partially annealed doped tubes with enhanced electrical conductivities could be used in the fabrication of robust and electrically conducting composites, and these results could
20 be extrapolated to N-doped graphene and other nanocarbons.

1. Introduction

The modification of the electronic and optical properties of carbon nanotubes via the introduction of nitrogen atoms into the nanotube sidewalls has been explored.[1-3] N atoms have been
25 incorporated into carbon nanotubes by the thermal decomposition of N containing compounds or vapor over metal nanoparticles at high temperatures.[4-17] The N-doped carbon nanotubes have showed metallic behavior, characterized by the presence of a donor state close to the Fermi level.[18-23] In addition, they may
30 have potential applications as efficient supporting materials for anchoring catalytic particles[24-26]; as catalysts for the oxygen reduction reaction in fuel cells[27-30]; as high-performance electron field emitters[20,31-33]; as a highly selective electron transport materials for solar cell[34]; and as a multifunctional filler in
35 polymeric composites[35-37]. In addition, the incorporation of N atoms is known to improve the biocompatibility of carbon nanotubes[38].

The unusual properties and potential applications of N-doped carbon nanotubes can be explained by the way N atoms are
40 bonded to C atoms on the sidewalls of nanotubes. It has been reported that the amount and type of N functionalities within N-doped carbon nanotubes could be controlled by varying the synthetic conditions, such as the reaction temperature, the type of catalyst and the feedstock.[39,40] Moreover, the electrical
45 conductivity of the bulk material is roughly proportional to the amount of N atoms incorporated in the structure.[17,21,23] Four types of N atoms have been identified in carbon nanotubes by X-ray photoelectron spectroscopy (XPS) studies: pyridinic, pyrrolic, quaternary and oxidized pyridinic N. When considering the
50 potential applications of N-doped multi-walled carbon nanotubes, it is essential to understand the effect of the different N functionalities on the electrical conductivity of individual carbon nanotubes, in order to tailor the N functionalities and thus control the electrical transport of the nanotubes.

55 In this paper, we report an approach able to tune both the content of N functionalities and the electrical conductivity via high-temperature thermal treatments. Specifically, as-grown N-doped multi-walled carbon nanotubes (N-MWNTs) were thermally treated at temperatures ranging between 1000 °C and 2000 °C in
60 argon and the variation in their electrical conductivity, at both the bulk and the individual tube scale, were correlated to the thermal stability of N functionalities. The quaternary N atoms (N bonded to three carbon atoms) were thermally stable up to 1500 °C. The individual nanotubes annealed at 1000 °C exhibited the lowest
65 electrical resistance, even lower to the values observed in highly crystalline nanotubes produced using an arc discharge.

2. Experimental details

The N-doped N-MWNTs were synthesized by the decomposition of a solution containing 2.5 wt % ferrocene and benzylamine
70 (97.5 wt %), as previously described.[41] The produced N-MWNTs

were then heat treated under an argon flow for 30 min at various temperatures, ranging from 1000 °C to 2000 °C, using a graphite furnace. Before heating, the graphite furnace was vacuumed (0.13 MPa) and then flushed with argon gas (1 L/min) in order to eliminate oxygen or exclude the possibility of oxidation in nanotube sample. The morphology and texture of the pristine and heat-treated tubes were characterized using scanning electron microscopy (SEM, JEOL JSM-6335Fs) and high-resolution transmission electron microscopy (HRTEM, CEOS Double Cs corrector equipped JEOL JEM-2100F, 120 kV). Raman spectra were collected using a T64000 Triple Raman Spectrometer (Horiba Jobin Yvon) with four different laser lines (488, 514, 633 and 785 nm), and the curve fitting was carried out using the Lorentzian distribution function. The electrical resistivity of N-MWNTs in the bulk state was measured using the four-point probe method (Mitsubishi Chemical, PD-51). The electrical resistance of an individual carbon nanotube was measured by the following procedure: a nanotube suspension was spin-coated on SiO_2 electrode, and the electrode patterns were formed by depositing tungsten (W) on an individual carbon nanotube by focused-ion-beam lithography (SMI2059, SII, Japan), in order to exclude the contact resistance between the carbon nanotube and the electrode. The intrinsic resistance was obtained from the linear current-voltage relationship from -1 to 1 V (Advantest, TR-6143).
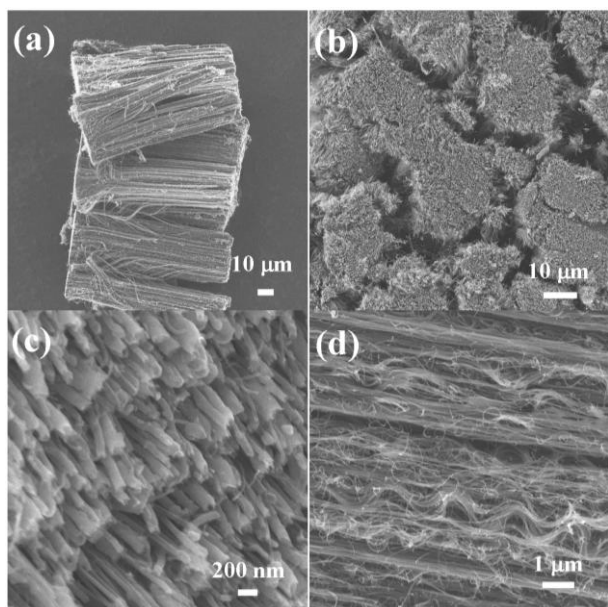
3. Results and discussion

Fig. 1 (a-d) SEM images of vertically aligned N-doped MWNTs at different angles and magnifications. Note that the tube ends are opened.

As-grown N-doped carbon nanotubes consisted of large bundles (Fig. 1 (a, b)) of aligned nanotubes (Fig. 1 (d)). In some cases, the ends of the tubes were open (Fig. 1 (c)). High-temperature thermal treatment was employed to modify both the surface functionalities and the degree of crystallinity within the carbon nanotubes. This heat treatment appears to be a powerful tool for improving their structural integrity, and could effectively remove trapped metallic impurities, particularly Fe below 20 ppm.[42-44] In

this particular study, as-grown N-MWNTs were thermally treated in argon at temperatures between 1000 °C and 2000 °C, using a graphite furnace.
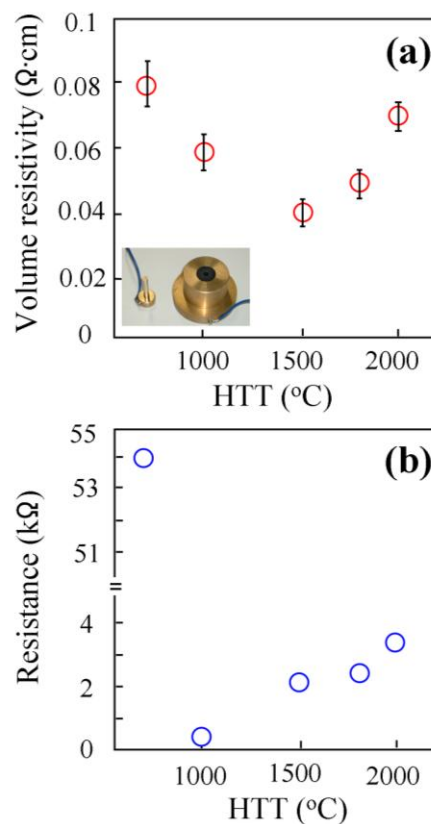

Fig. 2 (a) Variation in the volumetric resistivity of N-doped MWNTs as a function of heat treatment temperature at a density of 1.23 g/cm^3; the inset shows the sample holder. (b) Variation of the electrical resistance of an individual N-doped MWNT as a function of heat treatment temperature.

In order to understand the structural and electrical transport changes within our N-doped MWNTs, we measured the electrical resistivity in the bulk state using a four-point probe method (Fig. 2 (a)). A specific amount of the carbon nanotubes was placed in the sample holder (Fig. 2 (a), inset), and the resistivity at a nanotube mass density of 1.23 g/cm^3 was measured. In order to study conductivity changes induced by the Fe encapsulates, we have conducted bulk conductivity measurements of hydrochloric acid (HCl) treated N-doped MWNTs, and observed no significant change in the electrical resistance in bulk. Therefore, the Fe particles appear not to play a critical role in the electrical transport of the "metal-free" N-doped MWNTs. For tubes heat treated at below 1500 °C, a rapid decrease in electrical resistivity was observed, which can be explained by the removal of surface functional groups and aromatic hydrocarbons from the outer surface of the doped carbon nanotubes. However, for tubes heat treated above 1500 °C, a continuous increase in volumetric resistivity was detected. In addition, the electrical resistance of an individual tube was measured (Fig. 2 (b)). The intrinsic resistance of an individual tube was obtained from a linear current-voltage relationship up to 1 V. The lowest electrical resistance (0.5 kΩ) was observed in the tubes heat treated at 1000 °C, although tubes prepared at 2000 °C still exhibited a relatively low electrical
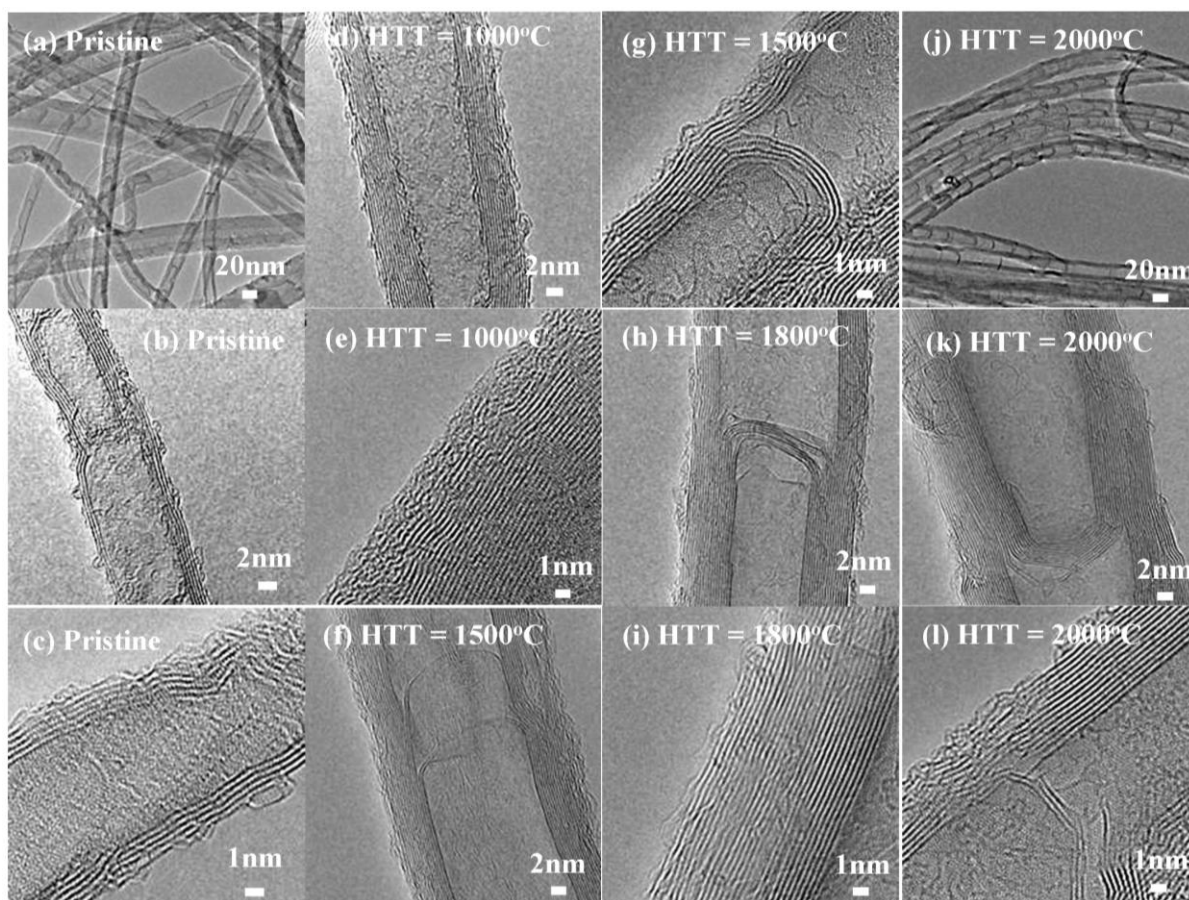
Fig. 3 HRTEM images of (a-c) pristine N-MWNTs and thermally annealed N-MWNTs, under an argon atmosphere, at (d, e) 1000 °C, (f, g) 1500 °C, (h, i) 1800 °C and (j-l) 2000 °C.
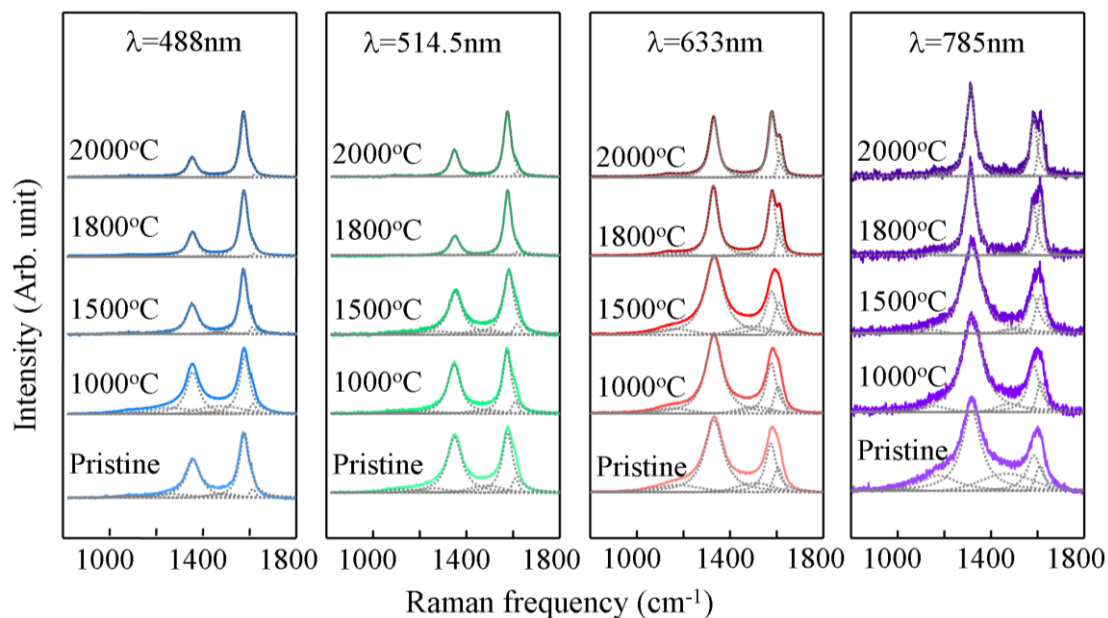

Fig. 4 Raman spectra of pristine N-doped MWNTs and thermally annealed N-doped MWNTs, in an argon atmosphere, at temperatures ranging between 1000 °C and 2000 °C, using four laser lines (488, 514.5, 633 and 785 nm).

resistance (3.5 kΩ). It is noteworthy that an arc-produced (pure carbon) MWNT has been reported to exhibit a resistance of 2.4 kΩ at room temperature.[45] Thus, the lowest electrical resistance value in our nanotubes arises from the partial content of N atoms (doping), which is consistent with several reported papers.[18-23] However, the increase in the electrical resistance of carbon
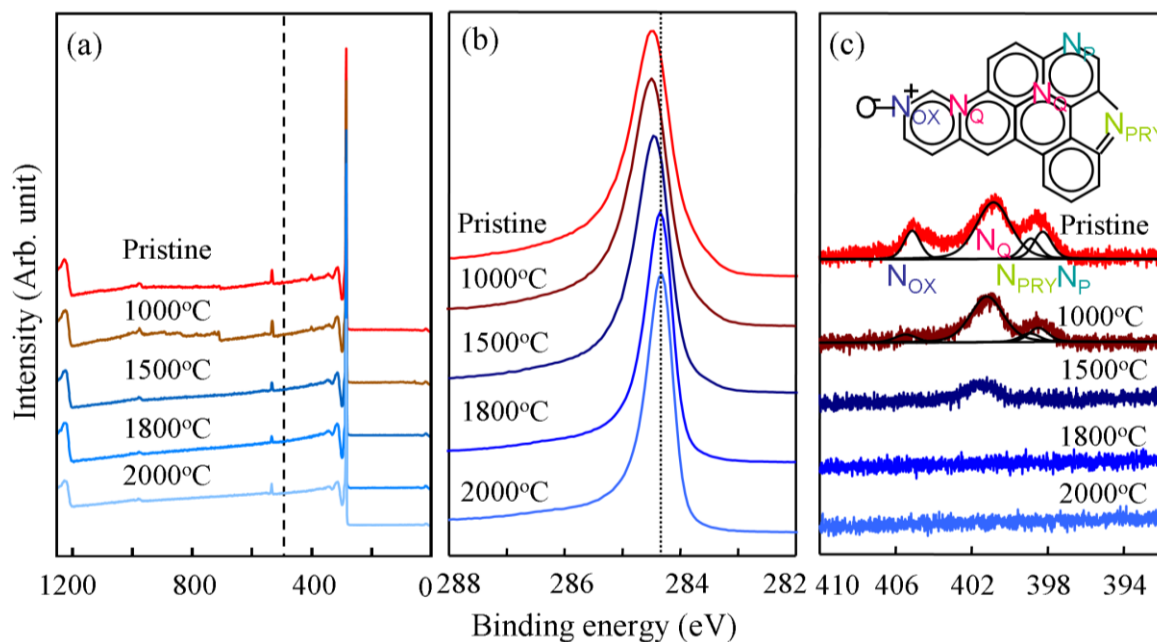
Fig. 5 XPS data of pristine N-doped MWNTs and thermally annealed N-doped MWNTs at temperatures ranging between 1000 °C and 2000 °C. (a) The wide-scan, (b) C 1s region and (c) N 1s region.

nanotubes that are thermally treated at temperatures ranging between 1500 °C and 2000 °C is not usually observed for undoped carbon nanotubes (Fig. S1). This increase in electrical resistivity and resistance for tubes at temperatures between 1500 °C and 2000 °C may be attributed to the absence of N atoms within the nanotubes. There are two opposing effects caused by high temperature thermal treatment which affect the electrical conductivity of N-doped carbon nanotubes: one is the improved structural integrity of the carbon nanotubes (enhanced degree of crystallinity), and the other is the change in concentrations and type of the N atoms incorporated within the hexagonal lattice of the tubes.

In order to obtain visual confirmation of the improved structural integrity, HR-TEM images of the pristine and the thermally treated tubes were obtained (see Fig. 3). As-grown nanotubes were long, linear, and exhibited a bamboo-like structure with regularly arranged compartments contained in a hollow core (Fig. 3 (a)). In addition, the graphene layers of the as-produced tubes were corrugated, indicating a low degree of structural crystallinity casued by the introduction of N atoms (Fig. 3 (b, c)). In this context, the introduction of N atoms into the graphitic layer is known to create pentagons which facilitate the formation of distorted or defective layers.[40,46] We noted a distinctive change in the HRTEM images for nanotubes that were thermally treated at 1000 °C and 1500 °C (Fig. 3 (d-g)). As the temperature was increased to 1800 °C and 2000 °C, the short, corrugated fringes became long, straight layers (Fig. 3 (h-l)), thus indicating an improvement in the structural integrity caused by the thermal annealing. In addition, the internal caps were transformed from round cap morphologies (Fig. 3 (g)) into more facetted caps (Fig. 3 (k)). This kind of morphological change is often seen at the tip of thermally treated nanotubes, [42-44] because the facetted structure is energetically more stable at high temperatures.

Raman spectra on the different samples were recorded using four laser lines (488, 514.5, 633 and 785 nm) (Fig. 4), and this analysis provides quantitative information about the near-surface region of carbon nanotubes.[47] There were two distinctive lines in the Raman spectra: the G-band (E_{2g2}) located at 1580 cm^{-1}, and the D-band (defect-induced mode) appearing at 1350 cm^{-1}. As the wavelength of the laser lines increased, the D-band became more intense and downshifted, in accordance with double resonance theory.[48] For N-MWNTs that were thermally treated below 1500 °C, there was no distinctive change in the Raman spectra. As the temperature increased from 1500 °C to 2000 °C, the half width at half maximum intensity of the G-band and the intensity of the D-band decreased, thus indicating that the defects were progressively removed upon thermal annealing.

The D'-band simultaneously appears in the Raman spectra of nanotubes thermally treated at 1800 °C and 2000 °C when using laser lines of 633 and 785 nm. In order to quantify the structural changes, the R value (I_D/I_G, the integrated intensity of the D band divided by the integrated intensity of the G band) was plotted as a function of the heat treatment temperature (Fig. S2); the R value has been previously used as an indicator of the crystalline structure of carbon materials, including carbon nanotubes.[49,50] For nanotubes heat treated at temperatures below 1500 °C, the presence of defects and surface functional groups decrease and some N atoms remain embedded in the hexagonal framework of the tubes. However, for the tubes treated at 1800 °C and 2000 °C, the defects are completely annealed by the high temperatures, and the presence of N dopant disappears (see XPS data below).

Finally, the surface functionalities of the doped nanotubes, and their stability at high temperatures were examined using XPS. The wide-scan XPS spectra of the as-grown tubes revealed peaks located at 284.4 eV (C 1s), 400 eV (N 1s) and 532.2 eV (O 1s) (Fig. 5 (a)). However, after a thermal treatment at 1800 °C, the intensity of the O 1s peaks decreased by a factor of 2, and the N 1s peak disappeared. In order to quantify these changes, the

atomic concentrations of carbon (C), oxygen (O) and N atoms are summarized in Table 1.

A consecutive decrease in the content of foreign atoms is observed as a function of the heat treatment temperature. This process increases the carbon content via the elimination of foreign atoms such as N, O and iron (Fe). The removal of Fe was observed in nanotubes treated at 1500 °C, whereas the elimination of N atoms was noted in nanotubes treated at 1800 °C. The residual O content in nanotubes treated above 1500 °C is probably arising from water physically adsorbed on the carbon materials or present in the XPS chamber. These changes were reflected in the C 1s spectra (Fig. 5 (b)). As the temperature increased, the peaks changed in shape from asymmetric to symmetric, and the full width at half maximum substantially decreased. Furthermore, the peaks were shifted to a lower binding energy, approching the energy of the sp^2 C-C bond of graphite. The N 1s spectra were magnified in order to identify the N functionalities, determine their thermal stability as a function of heat treatment temperature (Fig. 5 (c)). The N 1s peak was deconvoluted into four peaks: the peak located at 398.5 eV corresponds to pyridine-like N, the peak located at 400.1 eV from the pyrrolic N; the strong signal at 401.4 eV originated from the quaternary graphite-like N or substitutional N; and a weak peak located at 402-405 eV is assigned to an oxygenated N group.[51,52] When as-grown N-MWNTs (containing 2.7 at % of N) were thermally treated at 1000 °C, preferential evolution of the oxygenated N atoms was observed (N content of 0.78 at %; see Table 1), which resulted in a large decrease in the electrical resistance of the individual nanotubes from 54 kΩ to 0.5 kΩ. The majority of the pyridine-like N decomposed, whereas the quaternary N remained stable up to 1500 °C. For N-MWNTs heat treated at 1800 °C and 2000 °C, we could not identify N atoms. However, the detection limit of this XPS is ~0.1 atom %. Therefore, the observed electrical resistance for tubes treated at 1800 °C and 2000 °C, suggests that even a small number of N atoms below 0.1 atom % could be present within the nanotubes. Studies using second-ion mass spectroscopy are in progress in order to detect the residual N atoms within tubes that are thermally treated at 1800 °C and 2000 °C.

Table 1 Atomic composition of N-doped multi-walled carbon nanotubes thermally treated at various temperatures.

I.D.	Atomic composition (atom %)				Nitrogen functionality (%)			
	C	O	N	Fe	N_{OX}[a]	N_Q[b]	N_{PYR}[c]	N_P[d]
Pristine	89.4	7.7	2.7	0.17	13.3	62.1	9.2	15.4
HTT = 1000°C	90.1	8.8	0.78	0.35	6.0	72.8	8.2	13.0
HTT = 1500°C	96.1	3.6	0.32	-	-	100	-	-
HTT = 1800°C	96.7	3.3	-	-	-	-	-	-
HTT = 2000°C	97.1	2.9	-	-	-	-	-	-

[a] N_{OX} indicates oxidized group at 402-405 eV, [b] N_Q indicates quaternary nitrogen located at 401.4 eV, [c] N_{PRY} indicates pyrrolic nitrogen positioned at 400.1 eV, [d] N_P indicates pyridinic nitrogen present at 398.5 eV.

4. Conclusions

We have reported the temperature-dependent changes of the N functionalities and electrical conductivities of N-MWNTs that were thermally treated in argon at temperatures ranging between 1000 °C and 2000 °C. When as-grown N-doped nanotubes (containing 2.7 at % of N) were treated at 1000 °C, a substantial decrease in the electrical resistance, from 54 kΩ to 0.5 kΩ, was attributed to the removal of the oxygenated N atoms and surface groups (N content of 0.78 at %). At 1500 °C, the pyridine-like N decomposed, whereas the quaternary N remained stable (N content of 0.32 at %). Even though an enhanced degree of crystallinity was observed in N-MWNTs heat treated at 1800 °C and 2000 °C, verified by both the low R value in the Raman spectra and the presence of straight graphitic domains, the absence of the N atoms within the sidewall of tubes gave rise to a subtle increase in their electrical resistivity and resistance both at the bulk material and at the individual tube level. However, the low electrical resistance observed in individual tubes prepared at 1800 °C and 2000 °C, suggested that a small number of N atoms (below 0.1 atom %) could still be present within the nanotubes. Individual N-MWNTs heat treated at 1000 °C showed the lowest electrical resistance, caused by an an adequate concentration of pyridinic and quaternary N atoms, and could potentially be used as an effective supporting material for anchoring catalytic nanoparticles or as multifunctional fillers in polymeric composites.

Notes and references

[a] Faculty of Engineering, Shinshu University, 4-17-1 Wakasato, Nagano 380-8553, Japan. Fax: +81-26-269-5208; Tel: +81-26-269-5212; E-mail: yak@endomoribu.shinshu-u.ac.jp

[b] Carbon Institute of Science and Technology, Shinshu University, 4-17-1 Wakasato, Nagano 380-8553, Japan.

[c] Research Center for Exotic Nanocarbons (JST), Shinshu University, Wakasato 4-17-1, Nagano 380-8553, Japan.

[d] Department of Physics, Department of Materials Science and Engineering & Materials Research Institute, The Pennsylvania State University, 104 Davey Lab., University Park, PA 16802-6300, USA

† Electronic Supplementary Information (ESI) available: [Variations of electrical resistivity of undoped carbon nanotubes that are thermally treated at temperatures of 1000-2000 °C C in argon (Fig. S1), and Variations in the R value of carbon nanotubes which are thermally treated at 1000 and 2000 °C in argon (Fig. S2)]. See DOI: 10.1039/b000000x/

1 M. Terrones, A. Jorio, M. Endo, A. M. Rao, Y. A. Kim, T. Hayashi, H. Terrones, J.-C. Charlier, G. Dresselhaus, M. S. Dresselhaus, *Materials Today,* 2004, **7**, 30–45.

2. M. Terrones, A. G. Souza Filho, A. M. Rao, In Carbon Nanotubes: Advanced Topics in the Synthesis, Structure, Properties and Applications (Edited by A. Jorio, M. S. Dresselhaus, G. Dresselhaus), Springer, New York, 2008, 531–566.

3. P. Ayala, R. Arenal, M. Rummeli, A. Rubio, T. Pichler, *Carbon,* 2011, **48**, 575–586.

4. M. Terrones, A. M. Benito, C. Manteca-Diego, W. K. Hsu, O. I. Osman, J. P. Hare, D. G. Reid, H. Terrones, A. K. Cheetham, K. Prassides, H. W. Kroto, D. R. M. Walton, *Chem. Phys. Lett.*, 1996, **257**, 576–582.

5. T. Belz, A. Bauer, J. Find, M. Gunter, D. Herein, H. Mockel, N. Pfänder, H. Sauer, G. Schulz, J. Schütze, O. Timpe, U. Wild, R. Schlögi, *Carbon*, 1998, **36**, 731–741.

6. K. Suenaga, M. P. Johansson, N. Hellgren, E. Broitman, L. R. Wallenberg, C. Colliex, J. -E. Sundgren, L. Hultman, *Chem. Phys. Lett.*, 1999, **300**, 695–700.

7. M. Terrones, P. Redlich, N. Grobert, S. Trasobares, W. K. Hsu, H. Terrones, Y.Q. Zhu, J.P. Hare, C.L. Reeves, A. K. Cheetham, M. Rühle, H.W. Kroto, D.R.M. Walton, *Adv. Mater.*, 1999, **11**, 655–658.

8. M. Terrones, N. Grobert, H. Terrones, *Carbon*, 2002, **40**, 1665–1684.

9. Y. T. Lee, N. S. Kim, J. Park, J. B. Han, Y. S. Choi, H. Ryu, H. J. Lee, *Chem. Phys. Lett.*, 2003, **372**, 853–859.

10. M. Glerup, M. Castignolles, M. Holzinger, G. Hug, A. Loiseau, P. Bernier, *Chem. Commun.*, 2003, 2542–2543.

11. C. P. Ewels, M. Glerup, *J. Nanosci. Nanotechnol.*, 2005, **5**, 1345–1363.

12. A. G. Kudashov, A. V. Okotrub, L. G. Bulusheva, I. P. Asanov, Y. V. Shubin, N. F. Yudanov, L. I. Yudanova, V. S. Danilovich, O. G. Abrosimov. *J. Phys. Chem. B*, 2004, **108**, 9048–9053.

13. C. Tang, Y. Bando, D. Goldberg, F. Xu, *Carbon*, 2004, **42**, 2625–2633.

14. H. C. Choi, J. Park, B. Kim, *J. Phys. Chem. B*, 2005, **109**, 4333–4340.

15. S. Y. Kim, J. Lee, C. W. Na, J. Park, K. Seo, B. Kim, *Chem. Phys. Lett.*, 2005, **413**, 300–305.

16. S. van Dommele, K.P. de Jong, J. H. Bitter, *Chem. Commun.*, 2006, 4859–4861.

17. D. H. Lee, W. J. Lee, S. O. Kim, *Nano Lett.*, 2009, **9**, 1427–1432.

18. D. Tekleab, R. Czerw, D. L. Carroll, P. M. Ajayan, *Appl. Phys. Lett.,* 2000, **76**, 3594–3596.

19. R. Czerw, M. Terrones, J. C. Charlier, X. Blase, B. Foley, R. Kamalakaran, N. Grobert, H. Terrones, D. Tekleab, P. M. Ajayan, W. Blau, M. Ruehle, D. L. Carrol, *Nano Lett.*, 2001, **1**, 457–460.

20. D. Golberg, P. S. Dorozhkin, Y. Bando, Z. C. Dong, C. C. Tang, Y. Uemura, N. Grobert, M. Reyes-Reyes, H. Terrones, M. Terrones, *Appl. Phys. A-Mater.*, 2003, **76**, 499–507.

21. F. Villapando-Paez, A. Zamudio, A. L. Elias, H. Son, E. B. Barros, S. G. Chou, Y. A. Kim, H. Muramatsu, T. Hayashi, J. Kong, H. Terrones, G. Dresselhaus, M. Endo, M. Terrones, M. S. Dresselhaus, *Chem. Phys. Lett.*, 2006, **424**, 345–352.

22. W. J. Zhang, J. Y. Zhang, P. J. Li, X. Shen, Q. F. Zhang, J. L. Wu, *Nanotechnology*, 2008, **19**, 085202.

23. J. D. Wiggins-Camacho, K. J. Stevenson, Effect of Nitrogen Concentration on Capacitance, *J. Phys. Chem. C*, 2009, **113**, 19082–19090.

24. K. Jiang, L. S. Schadler, R. W. Siegel, X. J. Zhang, H. F. Zhang, M. Terrones, *J. Mater. Chem.*, 2004, **14**, 37–39.

25. K. Jiang, A. Eitan, L. S. Schadler, P. M. Ajayan, R. W. Siegel, N. Grobert, M. Mayne, M. Reyes-Reyes, H. Terrones, M. Terrones, *Nano Lett.*, 2003, **3**, 275–277.

26. A. Zamudio, A. L. Elias, J. A. Rodriguez-Manzo, F. Lopez-Urias, G. Rodriguez-Gattorno, F. Lupo, M. Ruhle, D. J. Smith, H. Terrones, D. Diaz, M. Terrones, *Small*, 2005, **2**, 346–350.

27. P. H. Matter, E. Wang, J. M. Millet, U. S. Ozkan, *J. Phys. Chem. C*, 2007, **111**, 1444–1450.

28. S. Maldonado, K. J. Stevenson, *J. Phys. Chem. B*, 2005, **109**, 4707–4716.

29. S. Kundu, T. C. Nagaiah, W. Xia, Y. Wang, S. van Dommele, J. H. Bitter, M. Santa, G. Grundmeier, M. Bron, W. Schuhmann, M. Muhler, *J. Phys. Chem. C*, 2009, **113**, 14302–14310.

30. K. Gong, F. Du, Z. Xia, M. Durstock, L. Dai, *Science*, 2009, **323**, 760–764.

31. M. Doytcheva, M. Kaiser, M. Reyes-Reyes, M. Terrones, N. de Jonge, *Chem. Phys. Lett.*, 2004, **396**, 126–130.

32. D. H. Lee, J. A. Lee, W. J. Lee, S. O. Kim, Small 2011, 7, 95–100.

33. D. H. Lee, J. E. Kim, T. H. Han, J. W. Hwang, S. J. S.-Y. Choi, S. H. Hong, W. J. Lee, R. S. Ruoff, S. O. Kim, *Adv. Mater.* 2010, **22**, 1247–1252.

34. J. M. Lee, J. S. Park, S. H. Lee, H. Kim, S. Yoo, S. O. Kim, *Adv. Mater.* 2011, **23**, 629–633.

35. B. Fragneaud, K. Masenelli-Varlot, A. Gonzalez-Montiel, M. Terrones, J. Y. Cavaille, *Chem. Phys. Lett.*, 2005, **419**, 567–573.

36. M. Dehonor, K. Masenelli-Varlot, A. Gonzalez-Montiel, C. Gauthier, J. Y. Cavaille, H. Terrones, M. Terrones, *Chem. Commun.*, 2005, 5349–5351.

37. B. Fragneaud, K. Masenelli-Varlot, A. Gonzalez-Montiel, M. Terrones, J. Y. Cavaille, *Chem. Phys. Lett.*, 2007, **444**, 1–8.

38. J. L. Carrero-Sanchez, A. L. Elias, R. Mancilla, G. Arellin, H. Terrones, J. P. Laclette, M. Terrones, *Nano Lett.*, 2006, **6**, 1609–1616.

39. S. van Dommele, A. Romero-Izqirdo, R. Brydson, K. P. de Jong, J. H. Bitter, *Carbon*, 2008, **46**, 138–148.

40. B. G. Sumpter, V. Meunier, J. M. Rome-Herrera, E. Cruz-Silva, D. A. Cullen, H. Terrones, D. J. Smith, M. Terrones, *ACS Nano*, 2007, **1**, 369–375.

41. M. Terrones, P. M. Ajayan, F. Banhart, X. Blase, D. L. Carroll, J. C. Charlier, R. Czerw, B. Foley, N. Grobert, R. Kamalakaran, P. Kohler-Redlich, M. Rühle, T. Seeger, H. Terrones, *Appl. Phys. A*, 2002, **74**, 355–361.

42. Y. A. Kim, K. Osada, T. Hayashi, M. Endo, M. S. Dresselhaus, *Chem. Phys. Lett.*, 2003, **380**, 319–324.

43. Y. A. Kim, T. Hayashi, M. Endo, Y. Kaburagi, T. Tsukada, J. Shan, K. Osato, S. Tsuruoka, *Carbon*, 2005, **43**, 2243–2250.

44. J. Chen, A. Kuno, M. Matsuo, T. Tsukada, T. Tamura, K. Osato, J. Y. Shan, F. Munekane, Y. A. Kim, T. Hayashi, M. Endo, *Carbon*, 2008, **46**, 391–396.

45. B. Q. Wei, R. Vajtai, P. M. Ajayan, *Appl. Phys. Lett.*, 2001, **79**, 1172–1174.

46. H. Sjostrom, S. Stafstrom, M. Boman, J. E. Sundgren, *Phys. Rev. Lett.*, 1995, **75**, 1336–1339.

47. M. S. Dresselhaus, G. Dresselhaus, R. Saito, A. Jorio, *Phys. Rep.*, 2005, **409**, 47–99.

48. R. Saito, A. Gruneis, G. G. Samsonideze, V. W. Brar, G. Dresselhaus, M. S. Dresselhaus, A. Jorio, L. G. Cancado, C. Fantini, M. A. Pimenta, A. G. Souza-Filho, *New. J. Phys.*, 2003, **5**, 157.

49. L. G. Cancado, K. Takai, T. Enoki, M. Endo, Y. A. Kim, H. Mizusaki, L. N. Coelho, R. Magalhaes Paniago, A. Jorio, and M. A. Pimenta, *Appl. Phys. Lett.*, 2006, **88**, 163106.

50. M. A. Pimenta, G. Dresselhaus, M. S. Dresselhaus, L. G. Cançado, A. Jorio and R. Saito, *Phys. Chem. Chem. Phys.*, 2007, **9**, 1276–1290.

51. E. Raymundo-Pinero, D. Cazorla-Amoros, A. Linares-Solano, J. Find, U. Wild, R. Schlogl, *Carbon*, 2002, **40**, 597–608.

52. J. R. Pels, F. Kapteijin, J. A. Moulijn, Q. Zhu, K. M. Thomas, *Carbon*, 1995, **33**, 1641–1653.